HHS Public Access

Author manuscript

Neuroscience. Author manuscript; available in PMC 2019 March 15.

Published in final edited form as:

Neuroscience. 2018 March 15; 374: 205–213. doi:10.1016/j.neuroscience.2018.01.054.

Nf2 mutation in Schwann cells delays functional neural recovery following injury

Kristy Truong[1], **Iram Ahmad**[1], **J. Jason Clark**[1], **Alison Seline**[1], **Tyler Bertroche**[1], **Brian Mostaert**[1], **Douglas J. Van Daele**[1], and **Marlan R. Hansen**[1,2]

[1]Department of Otolaryngology – Head and Neck Surgery, University of Iowa, Iowa City, Iowa, 52242

[2]Department of Neurosurgery, University of Iowa, Iowa City, Iowa, 52242

Abstract

Merlin is the protein product of the *NF2* tumor suppressor gene. Germline *NF2* mutation leads to neurofibromatosis type 2 (NF2), characterized by multiple intracranial and spinal schwannomas. Patients with NF2 also frequently develop peripheral neuropathies. While the role of merlin in SC neoplasia is well established, its role in SC homeostasis is less defined. Here we explore the role of merlin in SC responses to nerve injury and their ability to support axon regeneration. We performed sciatic nerve crush in wild type (WT) and in P0SchΔ39-121 transgenic mice that express a dominant negative *Nf2* isoform in SCs. Recovery of nerve function was assessed by measuring mean contact paw area on a pressure pad 7, 21, 60, and 90 days following nerve injury and by nerve conduction assays at 90 days following injury. After 90 days, the nerves were harvested and axon regeneration was quantified stereologically. Myelin ultrastructure was analyzed by electron microscopy. Functional studies showed delayed nerve regeneration in *Nf2* mutant mice compared to the WT mice. Delayed neural recovery correlated with a reduced density of regenerated axons and increased endoneurial space in mutants compared to WT mice. Nevertheless, functional and nerve conduction measures ultimately recovered to similar levels in WT and *Nf2* mutant mice, while there was a small (~17%) reduction in the percent of regenerated axons in the *Nf2* mutant mice. The data suggest that merlin function in SCs regulates neural ultrastructure and facilitates neural regeneration, in addition to its role in SC neoplasia.

Keywords

Merlin; Schwann cells; Sciatic nerve; Nerve regeneration; Axon-Schwann cell interaction

Correspondence: Marlan R. Hansen, MD, Department of Otolaryngology – Head and Neck Surgery, University of Iowa, Iowa City, Iowa 52242, marlan-hansen@uiowa.edu, Phone: (319) 353-7151, FAX: (319) 356-4547.

Introduction

Merlin (moesin-ezrin-radixin-like protein) is the protein product of the *NF2* tumor suppressor gene. Mutation of *NF2* results in the clinical tumor prone syndrome, neurofibromatosis type 2 (NF2), characterized by the development of multiple intracranial and spinal tumors, including schwannomas, meningioma, and ependymomas. Further, Schwann cell (SC)-specific mutation or deletion of *Nf2* in transgenic mice leads to the development of multiple schwannomas confirming that merlin functions as a tumor suppressor in SCs (Lee et al., 1997, Giovannini et al., 2000, Gehlhausen et al., 2015). In addition to tumor growth, patients with NF2 suffer from primary and injury-induced polyneuropathy (Grazzi et al., 1998, Schulz et al., 2014b).

Originally, compressive glial cell tumors or hyperproliferative SCs were assumed to account for the primary neuropathic symptoms developing in the course of NF2 (Grazzi et al., 1998, Schulz et al., 2014b). However, NF2-related neuropathy typically involves multiple peripheral nerves, appears in a symmetric and distal manner, occurs independently from the site of peripheral nerve schwannomas (Iwata et al., 1998, Sperfeld et al., 2002, Iseki et al., 2009) and may even develop years before tumors become evident (Sperfeld et al., 2002, Schulz et al., 2014b). These observations suggest a systemic, rather than focal, etiology. Further, neuropathological and electrophysiological investigations suggest that NF2-related polyneuropathy develops independently of schwannomas and likely involves axonal loss (Hagel et al., 2002, Sperfeld et al., 2002, Kuo et al., 2010, Baumer et al., 2013). Notably, merlin isoform-2 has been implicated in maintaining axonal integrity (Schulz et al., 2013) and loss of merlin function in neurons impairs functional nerve regeneration (Schulz et al., 2016) Taken together these observations suggest that polyneuropathy in NF2 patients can occur in the absence of schwannomas and that loss of merlin function in neurons likely impairs neural development, maintenance, and regeneration.

Merlin also plays an important role in SC development and SC-neuronal organization. It contributes to the control of SC numbers and is necessary for the correct organization and regulation of axo-glial heterotypic and glio-glial autotypic contacts such that mutation of *Nf2* in mice perturbs normal nerve development (Giovannini et al., 2000, Denisenko et al., 2008). Despite merlin's well-characterized role in SC and neural development, its subsequent contribution to SC responses to nerve injury remains largely unknown. In particular, the extent to which lack of functional merlin impacts neural regeneration following surgical trauma remains unknown. This is critical since patients with NF2 typically suffer multiple cranial and spinal neuropathies following microsurgical resection or radiosurgical treatment of cranial and spinal tumors. To address the influence of merlin function in the ability of SCs to support axon regeneration following nerve injury, we compared sciatic nerve regeneration in P0SchΔ39-121, which harbor a merlin mutation in SCs (Giovannini et al., 2000), and wild type (WT) mice using functional, electrophysiological and histological analysis. Our results indicate that merlin mutation results in myelination abnormalities and increased endoneurial space before and after nerve injury. Further, neural regeneration is delayed in mice lacking functional merlin in SCs but ultimately recover to the same extent as mice by functional, electrophysiological, and histological measures.

Experimental procedures

Mice

The total number of animals used in our study was 20. P0SchΔ39-121 transgenic mice were obtained from Riken Bioresource Center (Tsukuba, Japan). P0SchΔ39-121 heterozygous mice express a dominant negative form of merlin with an in-frame deletion of exons 2 and 3, mimicking pathological mutations found in NF2 patients (Giovannini et al., 1999, Giovannini et al., 2000). The expression of the transgene is limited to SCs since the gene is expressed under the control of a SC-specific P0 promoter. WT FVB mice were obtained from Jackson Labs (Bar Harbor, ME).

Surgery

Adult mice (3 months old) were anesthetized with ketamine/xylazine (40mg/kg; 5mg/kg, IP). A short incision was made overlying the quadriceps muscle in the right hind limb. Blunt dissection was performed to expose the sciatic nerve. Once isolated, the nerve was crushed for 30 seconds using a flat hemostatic forcep. The contralateral (left) nerves were uncrushed serving as controls. The use of animals and procedures performed were approved by the University of Iowa Institutional Animal Care and Use Committee.

Sciatic functional recovery

The animals (n=9 WT, n=11 P0SchΔ(39-121)) were followed for 90 days and functional recovery of sciatic nerve function prior to surgery at 7, 21, 60 and 90 days was assessed. We used the CatWalk XT (ver. 8, Noldus Information Technology, Wageningen, The Netherlands) system to study the functional recovery of the nerve. The method for conducting the CatWalk gain analysis has been described (Yang et al., 2012). Transit time and transit path parameters were set in the software and the mice were put on the walkway containing a pressure pad. The more pressure exerted, the larger the total area of skin-floor contact and thus the brighter the pixel. All areas containing pixels brighter than a pre-set threshold value were analyzed. The mean paw contact area and mean print area were determined for each step from each hind paw print (right and left side) and averaged for each run. Data were collected from three runs for each animal at each time point and averaged. The examiner was blind to genotype.

Nerve conduction testing

After exposing the affected nerve and prior to sacrifice 90 days after operation, nerve conduction velocity and amplitude testing were performed. A Grass neurostimulator was used to deliver stimuli starting with ten single electrical pulses followed by trains of pulses from 2 to 10 Hz. Stimulation electrodes were placed at the proximal end of the nerve and recording electrodes were placed at the distal end. Amplitude was kept constant during the testing and was the minimal current needed to induce a full action potential. Digital recordings at 50 kHz (using Windaq DI-720 hardware with Pro+ software) were made. The amplitude of the stimulation potential and the resultant distal nerve ending action potential was measured using the root mean square algorithm. The time from the beginning of the

stimulation potential to the beginning of the distal action potential representing the conduction velocity across the exposed nerve fiber was measured in microseconds.

Histology and Stereology

After completion of the electrophysiology, the sciatic nerves were dissected and 2-3 mm segments distal to the crush site on the injured side and an equivalent level on the uninjured mice were placed in freshly made 4% paraformaldehyde for at least 24 h. Samples were post-fixed in OsO4, dehydrated in an ethanol series, and embedded in Spurr's resin. For unbiased stereological analysis, a series of semithin sections (0.5μm) were stained with toluidine blue and images captured with a Leica DMR III microscope and CCD camera running Metamorph software (Molecular Devices, Inc., Sunnyvale, CA). Nerve fibers were counted using the 2D dissector method as described by Raimondo et al (Raimondo et al., 2009). A sampling grid containing multiple 1120 μm^2 circular counting frames was used. Counts were averaged from >5 sections per nerve.

For morphometric analyses, ultrathin sections (80-100 nm) were cut and placed on copper grids after verifying correct (transverse) orientation. Samples were then stained with uranyl acetate and lead citrate. Sections were viewed on a Jeol JEM 1230 transmission electron microscope (EM). Ten fields of view per nerve sample were selected randomly and digital electron micrographs were taken at 1000X. Using ImageJ software (NIH, Bethesda, MD), g-ratios were calculated on the EM micrographs as ratios of internal to external perimeters of the myelin sheath, creating a measure of myelin thickness. The examiner was blind to genotype.

Statistics

Differences among means for each group were analyzed by using t-tests and one way ANOVA using SigmaPlot software (Systat, San Jose, CA). We tested for and found normal distrubutions and equal variances in all sampled distrubutions with the exception of the data comparing percentage of endoneurial space. In this case, Mann Whitney Rank Sum Test was employed. A p value < 0.05 was considered significant.

Results

Nf2 mutation in SCs results in delayed neural recovery following injury

To begin to explore the role of merlin function on the ability of SCs to support axon regeneration, we performed right sciatic nerve crush injuries in WT and P0SchΔ39-121 mice. The left hindlimb was not manipulated. The CatWalk XT was used to measure hindpaw print area and mean contact area; both measures of limb function shown to be sensitive markers of functional recovery of the hind limbs following sciatic nerve injury (Supplementary videos 1–4) (Vogelaar et al., 2004). Mean contact area reflects the total surface area of the glass floor contacted by the paw at the moment of maximum paw-floor contact, a measure which reflects the load-bearing capacity of the limb. There was no significant difference in mean contact area ($t(19) = 0.37$, $p = 0.72$) in the uninjured nerves between WT (1.05 mm^2±0.35, mean±SEM) and P0SchΔ(39-121) (0.97 mm^2±1.61) mice (Fig. 1 A), suggesting normal neural function in P0SchΔ39-121 mice prior to injury. For

each mouse, the ratio of the right (injured) side to the left (uninjured) side print and mean contact areas was determined to account for differences in weight and other factors between animals, thereby having each mouse serve as its own control. Thus, for each measure, a ratio of 1 represents full function relative to the uninjured limb.

WT and P0SchΔ39-121 animals developed a severe functional deficit following sciatic nerve crush followed by evidence of neural recovery (Fig. 1A–B). Specifically, the mean contact area hindlimb ratios demonstrated an initial decrease at 7 days post-injury followed by a gradual recovery of function. By 90 days post-injury, the right and left hindlimb ratios for the mean contact area recovered to approximately one. In P0SchΔ39-121 mice (0.31 mm^2±0.09), the mean contact area of the injured paw remained significantly lower than in WT mice (0.69 mm^2±0.23) at 21 ($t(18) = 2.11$, $p=.049$) and 60 ($t(17) = 2.259$, 0.73 mm^2±0.23, 1.07 mm^2±0.355, $p=0.037$) days following injury, but recovered to a similar extent as in WT mice ($p=0.484$) at 90 days (Fig. 1A). This is further illustrated in Figure 1B. Thus, loss of merlin function in SCs delays functional recovery following nerve injury, yet the ultimate recovery does not appear to be adversely affected by the loss of merlin function.

Nf2 mutation in SCs does not result in a significant difference in conduction velocity or amplitude 90 days post-injury

Neural recovery was further examined by measuring the conduction velocity and amplitude, reflected by the root mean square, of the evoked compound action potential of the nerves 90 days following nerve injury using both single pulse and 2-10 Hz electrical stimulation (Table 1). Root mean square values did not differ between the stimulation electrode and the recording electrode between controls or any experimental condition. Similarly, there was no difference in the time difference between the stimulation potential and the resultant distal action potential for any control or experimental condition. This indicates there was no difference in stimulated nerve function between control or experimental conditions. The conduction velocity and amplitude of the compound action potential were similar for WT and P0SchΔ(39-121) mice 90 days following nerve injury, suggesting that loss of merlin function in SCs does not impair electrophysiological recovery 3 months following nerve injury.

Nf2 mutation in SCs results in reduced axon density before and after injury

Stereologic analyses were performed on stained nerve sections to determine whether *Nf2* mutation in SCs reduces the number of axons that regenerate following nerve injury. The 2D dissector method was used to quantify axon density and total number of myelinated fibers 90 days following nerve injury. There was a statistically significant decrease in axon density in the uninjured sciatic nerves of P0SchΔ(39-121) mice (12.6±1.89) compared to WT (22.9±0.59) mice ($t(8) = 3.694$, $p=0.006$) (Fig. 2A,B). Thus, even before injury, there is reduced axon density in mutant mice compared to WT mice. Likewise, at 90 days following nerve injury, there was a significant decrease in axon density in P0SchΔ(39-121) (12.4± 0.74) compared with WT (17.0±1.90) mice ($t(9) = 2.45$, 0.037)). Within WT mice, there is an absolute difference in myelin density before and after injury that approaches significance ($p=0.062$). The mutant mice show decreased baseline pre-injury myelin density that did not significantly change after injury ($p=0.908$). However, despite differences in axon

density with WT compared to mutant mice, no dramatic difference in the overall number of nerve fibers was found in the uninjured or the injured nerves. In P0SchΔ39-121 mice (1864±432), there is a slight decrease in total number of myelinated fibers following recovery from nerve injury compared to WT mice (2821±1052) but this difference was not statistically significant ($t(7) = 0.9$, $p=.42$). After crush, 93.5% of the total number of myelinated fibers in the injured limb compared to the uninjured limb were present in WT mice, whereas in the mutant mice only 76.4% of the number of fibers in the uninjured nerve were present in the injured nerve. This represents a 17.1% reduction in the degree of regeneration in P0SchΔ39-121 mice compared with WT mice.

Nf2 mutation in SCs results in thinner myelin sheaths and increased endoneurial space before and after injury

A decrease in axon density with preservation of the overall number of axons suggests that nerves in P0SchΔ39-121 have differences in myelin thickness and/or endoneurial space compared to nerves in WT mice. Transmission electron microscopy and light-microscopy revealed distinctive differences in uninjured nerves from P0SchΔ39-121 and WT mice (Figs. 2&3). For instance, uninjured nerves from *Nf2* mutated mice had an increased axon diameter (data not shown) that was statistically significant before and following nerve recovery with a decrease in myelin thickness compared to nerves from WT mice indicated by increased g-ratio value (Fig. 3A,B). Additionally, more double concentric myelin rings (Schmidt-Lanterman incisures, SLIs) were observed in the nerves from P0SchΔ39-121 mice compared to nerves from WT and the fibers in P0SchΔ39-121 often had an irregular shape compared to fibers in WT mice (Fig. 3A,C). Following nerve recovery, there was significant myelin thinning (increased gratio) in nerves from both WT (0.62±0.066) and P0SchΔ39-121 mice (0.71±0.03) compared to the uninjured nerves, with nerves from mutant mice (0.624±0.019) still showing significantly greater g-ratio ($F(3,9) = 73.32$, $p<0.001$) compared to WT mice (0.57±0.03). *Nf2* mutation in SCs also resulted in a higher number of SLIs in the myelin. The percentage of fibers with incisures were quantified for control and P0SchΔ39-121 mice before and after injury. We found the lowest value of SLIs before injury and after injury in the control group with controls prior to injury having 2%±2 (mean±SEM) and with control nerves after injury having 6.14%±3.33. We saw an increase in the number of incisures and the percentage of axons with incisures in P0SchΔ39-121 nerves pre- and post injury, with P0SchΔ39-121 nerves prior to injury having 31.25%±11.72 and P0SchΔ39-121 nerves post injury having 13.04%±8.65 (Fig. 3C); however, there is no significant difference detected between the control group and P0SchΔ39-121 group pre- ($p=0.12$) and post injury ($p=0.26$). These data indicate that P0SchΔ39-121 mice had significantly thinner and more variable myelin sheaths pre- and post-nerve injury.

Light microscopy analysis of semithin transverse sections showed an increase in the percentage of endoneurial space in nerves from P0SchΔ39-121 mice compared to WT mice in both normal and injured nerves (Fig. 2A,D). The endoneurial space comprised 75.8% ±1.20 (mean±SEM) of the endoneural space in P0SchΔ39-121 mice compared 42.6%±2.12 in WT mice ($p<0.001$). Following nerve injury, the P0SchΔ39-121 and WT mice experienced 1.3 fold and 1.8 fold increases in endoneurial space, respectively, with the nerves of P0SchΔ39-121 mice (81.8%±1.47) still being composed of a greater amount of

endoneurial space compared to nerves from WT (64.7%±1.06) mice ($F(3,20) = 29.68$, $p<0.001$).

Discussion

Lack of functional merlin in SCs delays neural regeneration

Despite merlin's well-characterized function as a tumor suppressor protein and its more recently recognized role in SC and neural development, its contribution to SC responses to nerve injury has remained largely unknown. We used a mouse model expressing a dominant-negative *Nf2* mutation in SCs to explore merlin's role in SCs' ability to support neural regeneration.

We found that neural recovery was delayed in mice lacking functional merlin in SCs compared to WT mice. The CatWalk system proved to be a valuable tool in assessing recovering of sciatic nerve function following injury. At both 21 and 60 days following nerve injury, P0SchΔ(39-121) mice displayed reduced mean contact area suggesting that merlin function in SCs facilitates nerve regeneration. Nevertheless, despite clear differences in nerve morphology and rate of functional recovery between the *Nf2* mutant and WT mice following crush injury, there was no significant difference in outcome associated with merlin mutation, as both the final electrophysiologic and functional measures were similar between groups. Delayed neural recovery in P0SchΔ39-121 mice is consistent with recent data that demonstrate that SCs that lack functional merlin exhibit defective SC responses to axonal damage, including cell proliferation. Nerve injury triggers rapid SC de-differentiation, myelin breakdown, and SC detachment from axons (Scherer and Salzer, 1997). Subsequently SCs differentiate, proliferate, and provide support for eventual axonal regrowth. Recent studies found that merlin becomes phosphorylated in SCs following axonal degeneration coincident with the SCs re-entry into the cell cycle (Provenzano et al., 2011, Ahmad et al., 2015). This phosphorylation inhibits the growth suppressive function of merlin and presumably thereby facilitates SC proliferation following nerve injury (Ahmad et al., 2015). Merlin acts as a tumor suppressor and suppresses pro-growth signaling events in response to contact inhibition (McClatchey and Giovannini, 2005, Okada et al., 2007, Schulz et al., 2010). Paradoxically, SC proliferation and apoptosis are reduced following axotomy in nerves from P0SchΔ39-121 mice compared to WT mice raising the possibility that phosphorylated merlin facilitates SC proliferation following nerve injury (Ahmad et al., 2015, Cheng and Hansen, 2016).

Nf2 mutation in SCs results in variations in neural structure before and after neural regeneration

Nf2 mutation in SCs resulted in structural alterations in the uninjured nerve and myelin sheath. For example, there was a higher density of myelinated axons in the uninjured nerves from WT mice compared with nerves from the *Nf2*-mutated mice. This difference appears to result from increased endoneurial space rather than a reduction of the number of myelinated fibers in the *Nf2* mutant mice; the overall number of myelinated fibers was similar for nerves from WT and mutant mice and there was increased endoneurial space in nerves from *Nf2* mutant mice compared to WT mice.

Myelin thickness was significantly reduced in uninjured and injured nerves from P0SchΔ39-121 mice compared their counterparts in WT mice, while myelin thickness was reduced following nerve recovery in WT mice compared to intact nerves. An increase in SLIs was also found in uninjured nerves from *Nf2* mutant mice compared to WT mice. Misshaped and dysmorphic nerve fibers were also observed in nerves from P0SchΔ39-121 compared to nerves from WT mice. These differences in axon density, morphology, and myelination persisted following recovery from nerve injury suggesting that merlin function in SCs plays a similar role in neural development and regeneration. Interestingly, a study by Guo suggests that myelin sheath organization and *in vitro* SC process number and morphology in Cdc42 mutant mice are merlin independent. However, their finding that radial sorting defect in Cdc42 mutants is rescued by *Nf2* mutation implies that WT merlin modulates SC radial sorting when Cdc42 is inactive (Guo et al., 2013).

In peripheral nerves, merlin associates with the cytoplasmic tail of paranodin/Caspr, an axonal transmembrane glycoprotein enriched at paranodal junctions and is important for reciprocal axo-glial signaling (Denisenko-Nehrbass et al., 2003). Merlin also interacts with βII-spectrin – another molecule supporting the axonal cytoskeleton at paranodes (Scoles et al., 1998, Chen et al., 2001, Salzer et al., 2008, Zhang et al., 2013). The increased number of SLIs seen in uninjured nerves from P0SchΔ39-121 compared to WT mice may result from disruption of merlin's role in assembling paranodal complexes. Merlin immunoreactivity has been reported in SLIs (Scherer and Gutmann, 1996), raising the possibility that the increase in SLIs in *Nf2* mutant mice results from the disruption of merlin's normal role in stabilizing cadherin-based adherens junctions (Lallemand et al., 2003). Additionally, merlin regulates other molecular interactions that control axon structure, organization, and maintenance and thereby may contribute to the morphologic differences seen nerves from P0SchΔ(39-121) compared to WT mice. For example, merlin regulates the expression and subcellular localization of ErbB receptors in SCs (Hansen et al., 2006, Lallemand et al., 2009, Ahmad et al., 2010, Schulz et al., 2014a). These receptors interact with neuregulin-1 on the axon surface to modulate SC proliferation, differentiation, and myelination (Fricker and Bennett, 2011, Ma et al., 2011, Schulz et al., 2014b).

NF2- related peripheral neuropathies

In addition to developing tumors of the peripheral and central nervous systems, patients with NF2 develop multiple peripheral neuropathies. Many of these neuropathies result from compressive tumors and nerve injuries (e.g. post-surgical) associated treatment of the tumors. However in addition to these tumor related neuropathies, NF2 patients also suffer neuropathies that appear independent of nerve sheath tumors and likely involve intrinsic defects in both neurons and SCs. For example, peripheral neuropathy occurs in individuals who bear mutations in just one merlin allele and in the absence of compressive nerve-damaging Schwann cell tumors (Hanemann et al., 2007, Schulz et al., 2014b). Sperfeld et al. (Sperfeld et al., 2002) suggest that polyneuropathy in NF2 patients occurs because SCs fail to properly adhere to, or ensheath, axons. Interestingly, sural nerve biopsies in patients with NF2-related peripheral neuropathy show decreased axon density (Sperfeld et al., 2002, Baumer et al., 2013) similar to the findings in P0SchΔ39-121 mice. Hagel et al. also provided evidence for pathological reduction of nerve fiber densities, accompanied by

diffuse proliferation of SCs in sural nerve biopsies suggesting a neural-intrinsic pathogenesis of neuropathy (Hagel et al., 2002). Two additional studies in patients with NF2-related peripheral neuropathy observed nerve conduction properties suggestive of axonal neuropathy (normal nerve conduction velocity with decreased compound muscle action potential) (Sperfeld et al., 2002, Baumer et al., 2013).

Significantly, merlin function in neurons appears to be essential for maintenance of axonal integrity and for normal axon regeneration following injury (Schulz et al., 2013, Schulz et al., 2016)Thus, loss of merlin function in axons represents a potential mechanism accounting for neuropathies in patients with NF2. The findings presented here in P0SchΔ39-121 mice demonstrate that *Nf2* mutation in SCs leads to defects in myelin structure and nerve regeneration. Thus defects in SCs that lack functional merlin, in addition to axonal intrinsic defects, may also contribute to neuropathies in NF2 patients, either primarily or following nerve injury. Taken together, these observations suggest that factors beyond tumor burden and local compression, including intrinsic problems in axons, SCs, or SC-axon interactions, contribute to the peripheral neuropathy in NF2 patients.

Conclusions

Our observations demonstrate that loss of merlin function in SCs leads to increased endoneurial space and ultrastructural myelin alterations in the sciatic nerve before and after injury. Further, loss of merlin function in SCs delays neural recovery following injury. Nevertheless, there were no significant functional or electrophysiological differences in neural regeneration attributable to *Nf2* mutation in SCs.

Supplementary Material

Refer to Web version on PubMed Central for supplementary material.

Acknowledgments

This study was supported by NIH grants NIH/NIDCD R01 DC009801, NIH/NIDCD P30 DC010362, NIH T32 DC000040 and grants from the AAO-HNS/PSF and American Otological Society.

References

Ahmad I, Fernando A, Gurgel R, Jason Clark J, Xu L, Hansen MR. Merlin status regulates p75(NTR) expression and apoptotic signaling in Schwann cells following nerve injury. Neurobiol Dis. 2015; 82:114–122. [PubMed: 26057084]

Ahmad Z, Brown CM, Patel AK, Ryan AF, Ongkeko R, Doherty JK. Merlin knockdown in human Schwann cells: clues to vestibular schwannoma tumorigenesis. Otol Neurotol. 2010; 31:460–466. [PubMed: 20195187]

Baumer P, Mautner VF, Baumer T, Schuhmann MU, Tatagiba M, Heiland S, Kaestel T, Bendszus M, Pham M. Accumulation of non-compressive fascicular lesions underlies NF2 polyneuropathy. J Neurol. 2013; 260:38–46. [PubMed: 22760943]

Chen Y, Yu P, Lu D, Tagle DA, Cai T. A novel isoform of beta-spectrin II localizes to cerebellar Purkinje-cell bodies and interacts with neurofibromatosis type 2 gene product schwannomin. J Mol Neurosci. 2001; 17:59–70. [PubMed: 11665863]

Cheng E, Hansen MR. Schwannomas provide insight into the role of p75(NTR) and merlin in Schwann cells following nerve injury and during regeneration. Neural Regen Res. 2016; 11:73–74. [PubMed: 26981085]

Denisenko-Nehrbass N, Goutebroze L, Galvez T, Bonnon C, Stankoff B, Ezan P, Giovannini M, Faivre-Sarrailh C, Girault JA. Association of Caspr/paranodin with tumour suppressor schwannomin/merlin and beta1 integrin in the central nervous system. J Neurochem. 2003; 84:209–221. [PubMed: 12558984]

Denisenko N, Cifuentes-Diaz C, Irinopoulou T, Carnaud M, Benoit E, Niwa-Kawakita M, Chareyre F, Giovannini M, Girault JA, Goutebroze L. Tumor suppressor schwannomin/merlin is critical for the organization of Schwann cell contacts in peripheral nerves. J Neurosci. 2008; 28:10472–10481. [PubMed: 18923024]

Fricker FR, Bennett DL. The role of neuregulin-1 in the response to nerve injury. Future Neurol. 2011; 6:809–822. [PubMed: 22121335]

Gehlhausen JR, Park SJ, Hickox AE, Shew M, Staser K, Rhodes SD, Menon K, Lajiness JD, Mwanthi M, Yang X, Yuan J, Territo P, Hutchins G, Nalepa G, Yang FC, Conway SJ, Heinz MG, Stemmer-Rachamimov A, Yates CW, Wade Clapp D. A murine model of neurofibromatosis type 2 that accurately phenocopies human schwannoma formation. Hum Mol Genet. 2015; 24:1–8. [PubMed: 25113746]

Giovannini M, Robanus-Maandag E, Niwa-Kawakita M, van der Valk M, Woodruff JM, Goutebroze L, Merel P, Berns A, Thomas G. Schwann cell hyperplasia and tumors in transgenic mice expressing a naturally occurring mutant NF2 protein. Genes Dev. 1999; 13:978–986. [PubMed: 10215625]

Giovannini M, Robanus-Maandag E, van der Valk M, Niwa-Kawakita M, Abramowski V, Goutebroze L, Woodruff JM, Berns A, Thomas G. Conditional biallelic Nf2 mutation in the mouse promotes manifestations of human neurofibromatosis type 2. Genes Dev. 2000; 14:1617–1630. [PubMed: 10887156]

Grazzi L, Chiapparini L, Parati EA, Giombini S, D'Amico D, Leone M, Bussone G. Type II neurofibromatosis presenting as quadriceps atrophy. Italian Journal of Neurological Sciences. 1998; 19:94–96. [PubMed: 10935844]

Guo L, Moon C, Zheng Y, Ratner N. Cdc42 regulates Schwann cell radial sorting and myelin sheath folding through NF2/merlin-dependent and independent signaling. Glia. 2013; 61:1906–1921. [PubMed: 24014231]

Hagel C, Lindenau M, Lamszus K, Kluwe L, Stavrou D, Mautner VF. Polyneuropathy in neurofibromatosis 2: clinical findings, molecular genetics and neuropathological alterations in sural nerve biopsy specimens. Acta Neuropathol. 2002; 104:179–187. [PubMed: 12111361]

Hanemann CO, Diebold R, Kaufmann D. Role of NF2 haploinsufficiency in NF2-associated polyneuropathy. Brain Pathol. 2007; 17:371–376. [PubMed: 17655741]

Hansen MR, Roehm PC, Chatterjee P, Green SH. Constitutive neuregulin-1/ErbB signaling contributes to human vestibular schwannoma proliferation. Glia. 2006; 53:593–600. [PubMed: 16432850]

Iseki C, Takahashi Y, Wada M, Kawanami T, Kurita K, Kato T. A case of neurofibromatosis type 2 (NF2) presenting with late-onset axonal polyneuropathy. Rinsho Shinkeigaku. 2009; 49:419–423. [PubMed: 19715170]

Iwata A, Kunimoto M, Inoue K. Schwann cell proliferation as the cause of peripheral neuropathy in neurofibromatosis-2. J Neurol Sci. 1998; 156:201–204. [PubMed: 9588858]

Kuo HC, Chen SR, Jung SM, Wu Chou YH, Huang CC, Chuang WL, Wei KC, Ro LS. Neurofibromatosis 2 with peripheral neuropathies: Electrophysiological, pathological and genetic studies of a Taiwanese family. Neuropathology. 2010

Lallemand D, Curto M, Saotome I, Giovannini M, McClatchey AI. NF2 deficiency promotes tumorigenesis and metastasis by destabilizing adherens junctions. Genes Dev. 2003; 17:1090–1100. [PubMed: 12695331]

Lallemand D, Manent J, Couvelard A, Watilliaux A, Siena M, Chareyre F, Lampin A, Niwa-Kawakita M, Kalamarides M, Giovannini M. Merlin regulates transmembrane receptor accumulation and signaling at the plasma membrane in primary mouse Schwann cells and in human schwannomas. Oncogene. 2009; 28:854–865. [PubMed: 19029950]

Lee JH, Sundaram V, Stein DJ, Kinney SE, Stacey DW, Golubic M. Reduced expression of schwannomin/merlin in human sporadic meningiomas. Neurosurgery. 1997; 40:578–587. [PubMed: 9055299]

Ma Z, Wang J, Song F, Loeb JA. Critical period of axoglial signaling between neuregulin-1 and brain-derived neurotrophic factor required for early Schwann cell survival and differentiation. J Neurosci. 2011; 31:9630–9640. [PubMed: 21715628]

McClatchey AI, Giovannini M. Membrane organization and tumorigenesis–the NF2 tumor suppressor, Merlin. Genes Dev. 2005; 19:2265–2277. [PubMed: 16204178]

Okada T, You L, Giancotti FG. Shedding light on Merlin's wizardry. Trends Cell Biol. 2007; 17:222–229. [PubMed: 17442573]

Provenzano MJ, Minner SA, Zander K, Clark JJ, Kane CJ, Green SH, Hansen MR. p75(NTR) expression and nuclear localization of p75(NTR) intracellular domain in spiral ganglion Schwann cells following deafness correlate with cell proliferation. Mol Cell Neurosci. 2011; 47:306–315. [PubMed: 21658451]

Raimondo S, Fornaro M, Di Scipio F, Ronchi G, Giacobini-Robecchi MG, Geuna S. Chapter 5: Methods and protocols in peripheral nerve regeneration experimental research: part II-morphological techniques. Int Rev Neurobiol. 2009; 87:81–103. [PubMed: 19682634]

Salzer JL, Brophy PJ, Peles E. Molecular domains of myelinated axons in the peripheral nervous system. Glia. 2008; 56:1532–1540. [PubMed: 18803321]

Scherer SS, Gutmann DH. Expression of the neurofibromatosis 2 tumor suppressor gene product, merlin, in Schwann cells. J Neurosci Res. 1996; 46:595–605. [PubMed: 8951671]

Scherer, SS., Salzer, JL. Axon–Schwann cell interactions during peripheral nerve degeneration and regeneration. In: Jessen, KR., Richardson, WD., editors. Glial Cell Development: basic principles and clinical relevance. 1997. p. 165-196.

Schulz A, Baader SL, Niwa-Kawakita M, Jung MJ, Bauer R, Garcia C, Zoch A, Schacke S, Hagel C, Mautner VF, Hanemann CO, Dun XP, Parkinson DB, Weis J, Schroder JM, Gutmann DH, Giovannini M, Morrison H. Merlin isoform 2 in neurofibromatosis type 2-associated polyneuropathy. Nat Neurosci. 2013; 16:426–433. [PubMed: 23455610]

Schulz A, Buttner R, Toledo A, Baader SL, von Maltzahn J, Irintchev A, Bauer R, Morrison H. Neuron-Specific Deletion of the Nf2 Tumor Suppressor Impairs Functional Nerve Regeneration. PLoS One. 2016; 11:e0159718. [PubMed: 27467574]

Schulz A, Geissler KJ, Kumar S, Leichsenring G, Morrison H, Baader SL. Merlin inhibits neurite outgrowth in the CNS. J Neurosci. 2010; 30:10177–10186. [PubMed: 20668201]

Schulz A, Kyselyova A, Baader SL, Jung MJ, Zoch A, Mautner VF, Hagel C, Morrison H. Neuronal merlin influences ERBB2 receptor expression on Schwann cells through neuregulin 1 type III signalling. Brain. 2014a; 137:420–432. [PubMed: 24309211]

Schulz A, Zoch A, Morrison H. A neuronal function of the tumor suppressor protein merlin. Acta Neuropathol Commun. 2014b; 2:82. [PubMed: 25012216]

Scoles DR, Huynh DP, Morcos PA, Coulsell ER, Robinson NG, Tamanoi F, Pulst SM. Neurofibromatosis 2 tumour suppressor schwannomin interacts with betaII-spectrin. Nat Genet. 1998; 18:354–359. [PubMed: 9537418]

Sperfeld AD, Hein C, Schroder JM, Ludolph AC, Hanemann CO. Occurrence and characterization of peripheral nerve involvement in neurofibromatosis type 2. Brain. 2002; 125:996–1004. [PubMed: 11960890]

Vogelaar CF, Vrinten DH, Hoekman MF, Brakkee JH, Burbach JP, Hamers FP. Sciatic nerve regeneration in mice and rats: recovery of sensory innervation is followed by a slowly retreating neuropathic pain-like syndrome. Brain Res. 2004; 1027:67–72. [PubMed: 15494158]

Yang DY, Sheu ML, Su HL, Cheng FC, Chen YJ, Chen CJ, Chiu WT, Yiin JJ, Sheehan J, Pan HC. Dual regeneration of muscle and nerve by intravenous administration of human amniotic fluid-derived mesenchymal stem cells regulated by stromal cell-derived factor-1alpha in a sciatic nerve injury model. J Neurosurg. 2012; 116:1357–1367. [PubMed: 22503125]

Zhang C, Susuki K, Zollinger DR, Dupree JL, Rasband MN. Membrane domain organization of myelinated axons requires betaII spectrin. J Cell Biol. 2013; 203:437–443. [PubMed: 24217619]

Highlights

- *Nf2* mutation in Schwann cells (SCs) results in delayed neural recovery as measured by the Cat Walk
- *Nf2* mutation in SCs results in reduced axon density but does not result in a significant reduction in axon regeneration.
- *Nf2* mutation in SCs results in a significant increase in extracellular matrix deposition.
- *Nf2* mutation in SCs does not result in a significant difference in conduction velocity or amplitude 90 days post-injury.

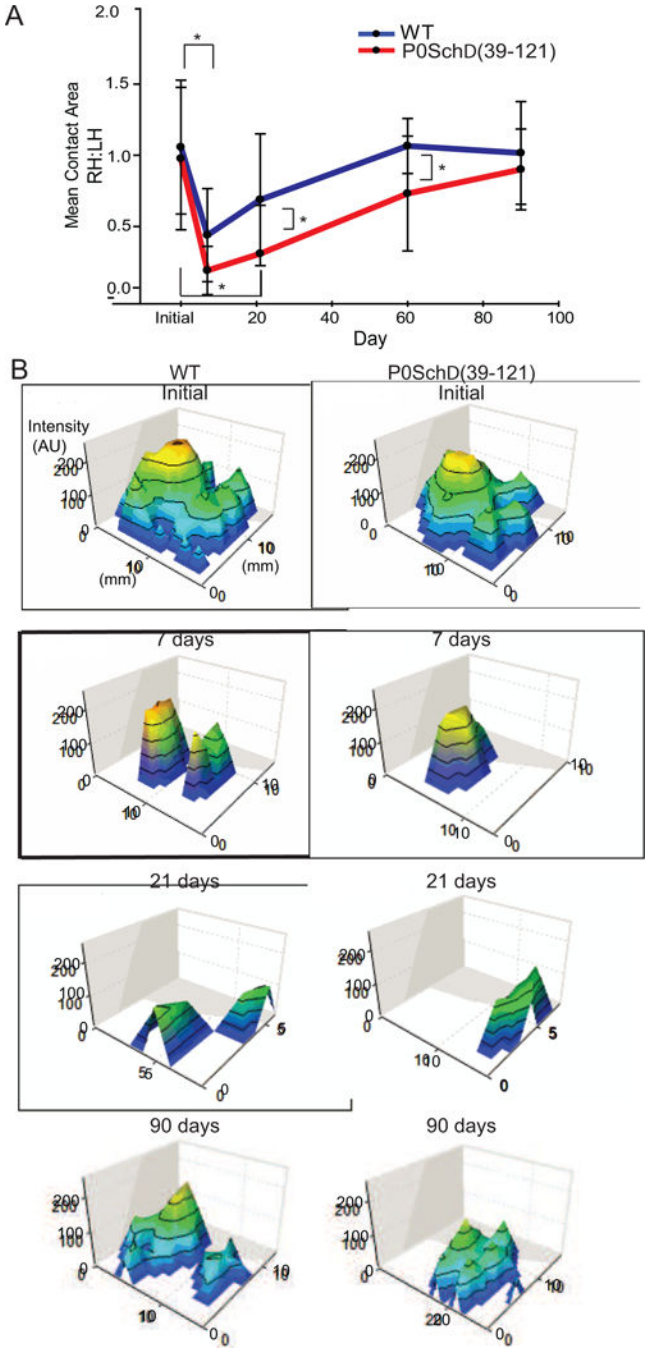

Figure 1.

Nf2 mutation in Schwann cells results in delayed nerve recovery following injury. CatWalk analysis in mice. A and B. Mean contact area of control group paws (blue) and P0SchΔ39-121 group paws (red) shown as a ratio of the contralateral paws during the follow-up period of 90 days. B. Representative 3D footprint intensity (expressed in arbitrary units, a.u.) tab plots of the right hind paw of the initial, 7 day, 21 day and 90 day time points. Data analysis was performed with a threshold value of 40 (arbitrary units, possible range 0-225), i.e. all pixels brighter than 40 are used. The color was representative of increased

density from green to yellow. Green color demonstrated low density and yellow color depicted high density. For each crossing of an animal, the mean was calculated per paw for contact area and print area. Mean values for all separate parameters were then calculated for each treatment group. Significant differences were found between the control group or P0SchΔ39-121 group and between time of testing by t-testing with normal distributions and equal variances. Error bars: ± SEM; * $p < 0.05$.

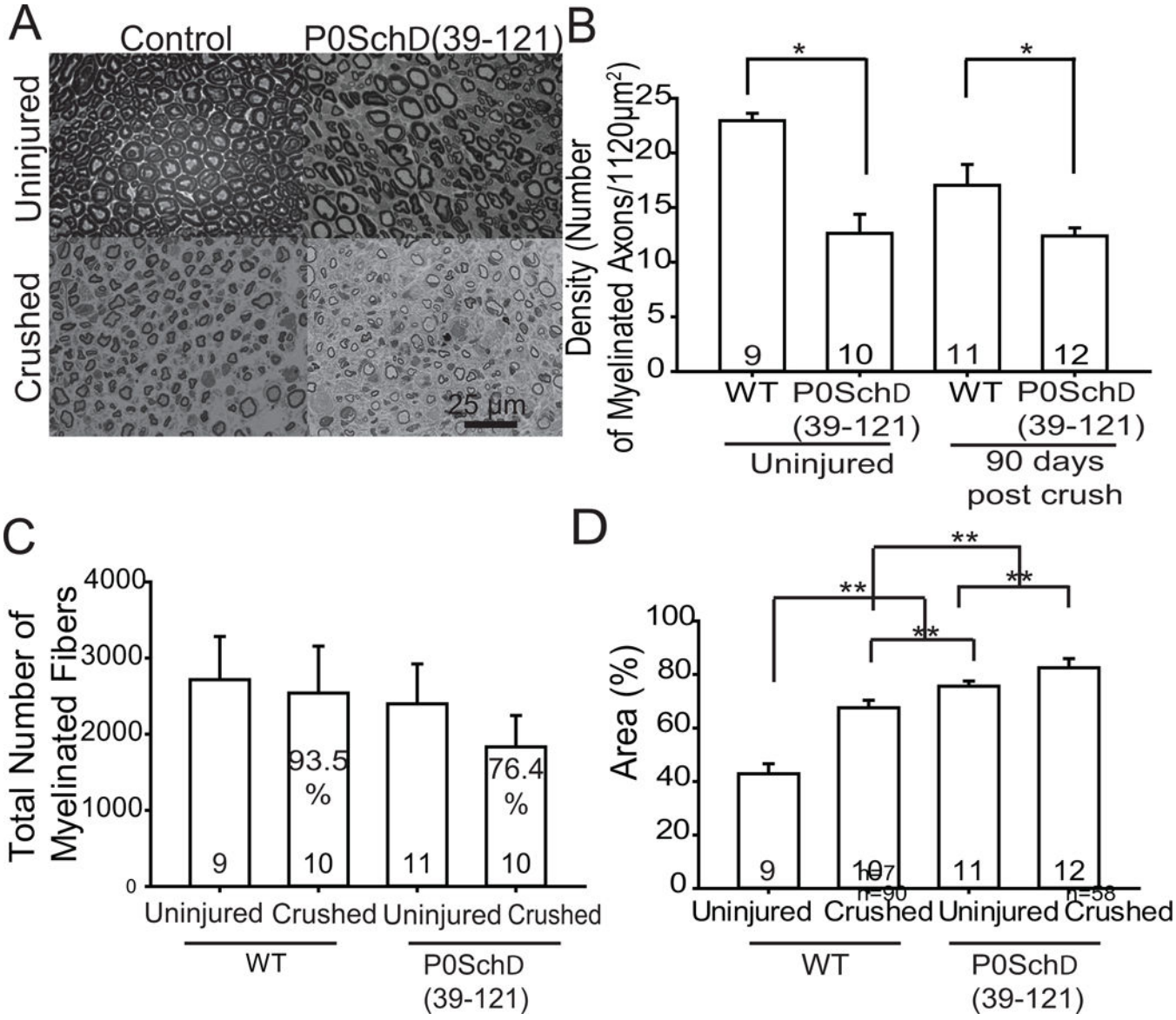

Figure 2.

Nf2 mutation in Schwann cells results in reduced axon density before injury and increases perineural space in nerves before and after injury. A. Semi-thin cross-sections of adult WT and P0SchΔ39-121 sciatic nerves. B. Quantification of axon density in sciatic nerves from WT and P0SchΔ39-121 mice. There was a significant decrease in axon density in uninjured nerves and in injured nerves following regeneration from P0SchΔ39-121 mice compared to WT mice. Within WT mice there is an absolute difference in myelin density before and after injury that is not significant. The mutant mice show decreased baseline pre-injury myelin density that did not significantly change after injury. n= total number of mice per group. C. Quantification of the total number of myelinated fibers per nerve in both uninjured and crushed in the WT and mutant mouse. No dramatic alteration of the number of fibers was found. In P0SchΔ39-121 mice, there is a slight decrease in total number of myelinated fivers compared to WT mice, but in general the number of myelinated axons in adult nerves were

similar in control and mutant mice. D. Average percent of endoneurial space for WT and P0SchΔ39-121 mice in uninjured nerve and nerves 90 days after crush injury. ** $p<0.001$ by one-way ANOVA with a post hoc Holm-Sidak test compared to each other condition (i.e. all conditions were significantly different from each other). n= total number of mice per group.

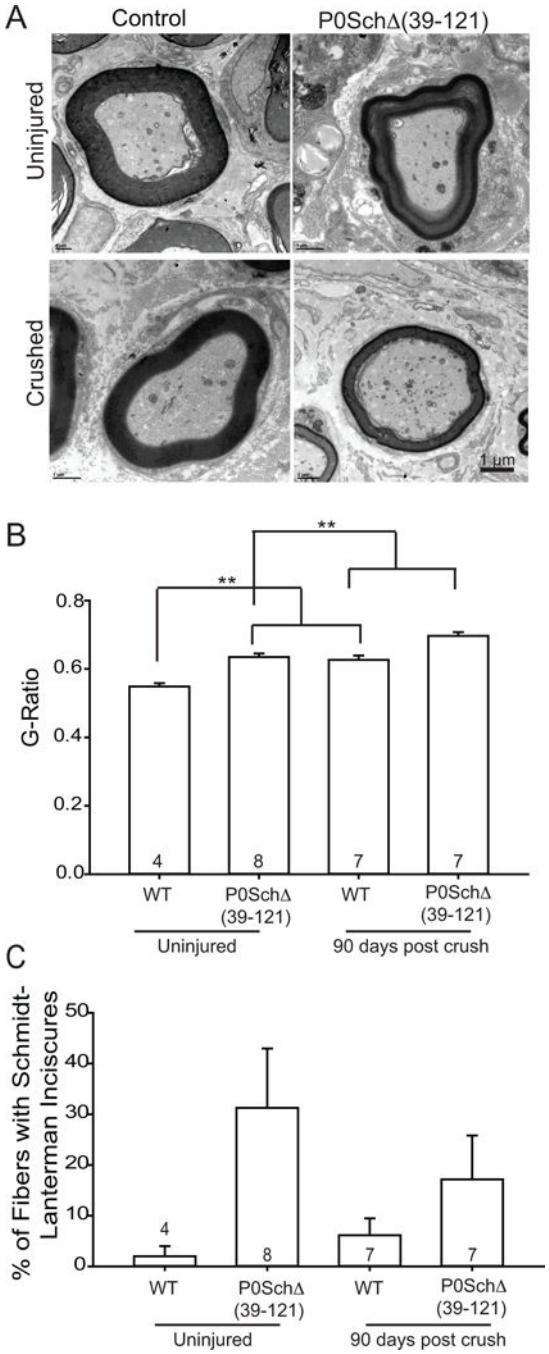

Figure 3.

Nf2 mutation in Schwann cells reduces myelin thickness and increases Schmidt-Lanterman incisures. A. Electron micrographs from sciatic nerve transverse sections from WT mice compared with P0SchΔ39-121 mice shows thinner myelin produced by P0SchΔ39-121 mice than normal control mice. The presence of concentric myelin rings corresponding to Schmidt-Lanterman incisures (SLIs, white arrow) is shown in nerves from P0SchΔ39-121 mice with demonstrative thin myelin sheaths associated with a higher g ratio seen in the axons on the periphery of the picture (shown in black arrow). Scale bar 1 μm. B.

Quantitation of myelin g-ratios. The g-ratio was increased in myelinated axons from P0SchΔ39-121 mice compared with WT mice before injury and 90 days post crush (**p<0.001 for both time points, ANOVA). n=total number of mice per group. C. Quantification of the percentage of fibers with SLIs. n=total number of fibers counted. Mutation of *Nf2* in SCs also resulted in a higher number of SLIs in the myelin pre- and post injury but was not significant (p values > 0.05 by Student's t-test).

Table 1

Nerve conduction studies

	Conduction velocity (m/sec)			Root mean square		
	WT	**P0SchΔ39-121**	**p value***	**WT**	**P0SchΔ39-121**	**p value***
	0.0979	0.0774	0.827513	0.11	0.03	0.663698
	0.0966	0.0985		0.1	0.09	
	0.1334	0.102		0.07	0.1	
	0.1028	0.0981		0.1	0.11	
	0.1026	0.1047		0.1	0.1	
	0.0903	0.1391		0.03	0.09	
	0.1028	0.1009		0.11	0.07	
	0.102	0.1007		0.1312	0.11	
Mean	**0.1046**	**0.10268**		**0.0939**	**0.0875**	

*Student's t-test